

# **Experiment 7:**

## **Waves on a Vibrating String**

**Name:** Omar Ozgur

**Date:** November 23, 2015 (11/23/15)

**Lab:** Section 1, Monday 9am

**TA:** Hector Garcia

**Lab Partner(s):** Christie Matthews, Fiona Guo

# Introduction

The purpose of this experiment was to explore the properties of mechanical waves that travel along a string. This involved predicting and measuring wave speeds based on different linear mass densities, as well as finding drive frequencies that would produce a series of harmonics.

Before beginning the experiment, the mass “ $M_0$ ” and total length “ $\ell_t$ ” of a piece of elastic string was recorded. This string was then suspended parallel to the table’s surface by attaching one end to a clamp, and draping the other end over a pulley. By attaching various weights to the free end of the string, the linear mass density could be changed. By relating the mass density “ $\mu$ ” to the tension “ $T$ ” on the string, the wave speed “ $v$ ” could be predicted.

The first step in calculating the mass density is to find the unstretched length “ $\ell_u$ ” of the section of string ahead of the clamp. This value can be calculated by subtracting the length of the excess string behind the clamp “ $\ell_e$ ” from the total length “ $\ell_t$ ” with equation 1.0. The uncertainty can be calculated with equation 1.2, which is based on the individual uncertainty values of the lengths that are used.

$$\ell_u = \ell_t - \ell_e \quad (\text{Eq. 1.0})$$

$$\text{If } f = x - y: \quad \delta f = \sqrt{(\delta x)^2 + (\delta y)^2} \quad (\text{Eq. 1.1})$$

$$\delta \ell_u = \sqrt{(\delta \ell_t)^2 + (\delta \ell_e)^2} \quad (\text{Eq. 1.2})$$

Since the unstretched length of string “ $\ell_u$ ” involved in the experiment is smaller than the total length “ $\ell_t$ ” of the string. The relationship between these values, along with the total mass “ $M_0$ ” of the string, can be used in equation 1.3 to calculate the mass “ $M$ ” of the string that is allowed to stretch based on applied tension. The uncertainty in “ $M$ ” can be found with equation 1.5.

$$M = M_0 \left( \frac{\ell_u}{\ell_t} \right) \quad (\text{Eq. 1.3})$$

$$\text{If } f = x * y: \quad \frac{\delta f}{|f_{best}|} = \sqrt{\left( \frac{\delta x}{|x_{best}|} \right)^2 + \left( \frac{\delta y}{|y_{best}|} \right)^2} \quad (\text{Eq. 1.4})$$

$$\delta M = |M_{best}| \sqrt{\left( \frac{\delta M_0}{|M_0_{best}|} \right)^2 + \left( \frac{\delta \left( \frac{\ell_u}{\ell_t} \right)}{\left| \left( \frac{\ell_u}{\ell_t} \right)_{best} \right|} \right)^2}$$

$$\begin{aligned}
&= |M_{best}| \sqrt{\left(\frac{\delta M_0}{|M_{0best}|}\right)^2 + \left(\frac{\left|\left(\frac{\ell_u}{\ell_t}\right)_{best}\right| \sqrt{\left(\frac{\delta \ell_u}{|\ell_{ubest}|}\right)^2 + \left(\frac{\delta \ell_t}{|\ell_{tbest}|}\right)^2}}{\left|\left(\frac{\ell_u}{\ell_t}\right)_{best}\right|}\right)^2} \\
&= |M_{best}| \sqrt{\left(\frac{\delta M_0}{|M_{0best}|}\right)^2 + \left(\frac{\delta \ell_u}{|\ell_{ubest}|}\right)^2 + \left(\frac{\delta \ell_t}{|\ell_{tbest}|}\right)^2} \quad (\text{Eq. 1.5})
\end{aligned}$$

In order to calculate the mass density of the string based on applied tension, the length “ $\ell_s$ ” of the stretched portion of string should be measured. The relationship between the stretched length and the mass “ $M$ ” of that section of string can be used in equation 1.6 to find the mass density “ $\mu$ ”. The uncertainty can be calculated by using equation 1.8, which is based on the uncertainty of the mass and length that is used. This mass density must be recalculated whenever the tension changes in order to account in the changing string length. If more tension is applied, the string will stretch more, causing a smaller mass density to be calculated. Contrarily, if less tension is applied, the string will stretch less, causing a larger mass density to be calculated.

$$\mu = \frac{M}{\ell_s} \quad (\text{Eq. 1.6})$$

$$\text{If } f = \frac{x}{y}: \quad \frac{\delta f}{|f_{best}|} = \sqrt{\left(\frac{\delta x}{|x_{best}|}\right)^2 + \left(\frac{\delta y}{|y_{best}|}\right)^2} \quad (\text{Eq. 1.7})$$

$$\delta \mu = |\mu_{best}| \sqrt{\left(\frac{\delta M}{|M_{best}|}\right)^2 + \left(\frac{\delta \ell_s}{|\ell_{sbest}|}\right)^2} \quad (\text{Eq. 1.8})$$

In order to determine the wave speed, the tension “ $T$ ” that causes the string to stretch must be calculated. This involves finding the tension “ $T_w$ ” based on the weight that is used, as well as the tension “ $T_h$ ” based on the portion of the string that hangs down from the pulley, since the string is not massless. The tension “ $T_w$ ”, along with its uncertainty, can be calculated with equations 1.9 and 2.0 based on gravitational acceleration “ $g$ ” and the recorded mass “ $m$ ” of the weight that is used.

$$T_w = mg \quad (\text{Eq. 1.9})$$

$$\delta T_w = |g|(\delta m) \quad (\text{Eq. 2.0})$$

The tension “ $T_h$ ” due to the hanging length of string, along with its uncertainty, can be calculated with equations 2.1 and 2.3 based on gravity “ $g$ ”, the mass “ $M$ ” of the stretched string, and the ratio of the hanging length “ $\ell_h$ ” of the string to the total stretched length “ $\ell_s$ ”.

$$T_h = \frac{\ell_h}{\ell_s} (M)(g) \quad (\text{Eq. 2.1})$$

$$\text{If } f = Ax: \quad \delta f = |A| \delta x \quad (\text{Eq. 2.2})$$

$$\delta T_h = |M||g||T_{h_{best}}| \sqrt{\left(\frac{\delta \ell_h}{|\ell_{h_{best}}|}\right)^2 + \left(\frac{\delta \ell_s}{|\ell_{s_{best}}|}\right)^2} \quad (\text{Eq. 2.3})$$

The sum of tensions “ $T_w$ ” and “ $T_h$ ” yields the total tension “ $T$ ” that is applied to the string. This value, along with its uncertainty, can be calculated by using equations 2.4 and 2.5 below.

$$T = T_w + T_h \quad (\text{Eq. 2.4})$$

$$\delta T = \sqrt{(\delta T_w)^2 + (\delta T_h)^2} \quad (\text{Eq. 2.5})$$

The wave speed can be calculated with equation 2.6 based on the total tension “ $T$ ” that is applied to the string, as well as the mass density “ $\mu$ ” that is updated to reflect the applied tension. The uncertainty can be found by using equation 2.8 below, which is based on the uncertainty in the determination of “ $T$ ” and “ $\mu$ ”.

$$v = \sqrt{\frac{T}{\mu}} \quad (\text{Eq. 2.6})$$

$$\text{If } f = Ax^n: \quad \frac{\delta f}{|f_{best}|} = |n| \frac{\delta x}{|x_{best}|} \quad (\text{Eq. 2.7})$$

$$\delta v = \left| \frac{1}{2} \right| \frac{\delta \left( \frac{T}{\mu} \right)}{\left| \left( \frac{T}{\mu} \right)_{best} \right|} = \frac{1}{2} \frac{\left| \left( \frac{T}{\mu} \right)_{best} \right| \sqrt{\left( \frac{\delta T}{|T_{best}|} \right)^2 + \left( \frac{\delta \mu}{|\mu_{best}|} \right)^2}}{\left| \left( \frac{T}{\mu} \right)_{best} \right|} = \frac{1}{2} \sqrt{\left( \frac{\delta T}{|T_{best}|} \right)^2 + \left( \frac{\delta \mu}{|\mu_{best}|} \right)^2} \quad (\text{Eq. 2.8})$$

In order to determine the wave speed “ $v$ ” based on experimental data, a laser pointer was used to illuminate the top of the string near close to the pulley, and a photodetector was pointed downward over the string to measure the intensity of the light. Whenever a wave caused the string to oscillate, the recorded light intensity changed accordingly. The changing light intensity

was recorded by using a data acquisition system, and this data was plotted in order to view repeating wave patterns.

By relating the distance “d” that the waves traveled to the change in time “ $\Delta t$ ” between two wave occurrences, the wave speed could be calculated based on two wave cycles. The wave speed of a particular trial could be found by taking the average of the wave speeds that were calculated based on many wave cycles, which is shown in equation 2.9. The uncertainty “ $\delta v$ ” in the measured wave speed values could be found by using equation 3.0, which relates each calculated wave speed value to the average value. In order to minimize uncertainty, it is important to use as much reliable data as possible.

$$v = \left( \frac{d}{\Delta t} \right)_{avg} \quad (\text{Eq. 2.9})$$

$$\delta v = \frac{1}{\sqrt{n}} \sqrt{\frac{1}{n-1} \sum_{i=1}^n (v_i - v_{best})^2} \quad (\text{Eq. 3.0})$$

Another part of the experiment involved analyzing light intensity amplitudes and generating Lissajous figures to calculate mode frequencies for standing waves generated by a wave driver. By increasing the driving frequency, different standing waves could be created so that clear nodes could be seen along the string.

## Experimental Results and Data Analysis



**Figure 1 Experiment Setup:** During this experiment, a length of elastic string was elevated parallel to a table’s surface by clamping one end, and draping the other end around a pulley. The addition of weights to the free end of the string caused the string to stretch, which affected its mass density, as well as the wave speed of propagating waves. In order to record data, a laser beam was used to illuminate the top of the string near the pulley, and a photodetector monitored the intensity of light that was scattered towards it. To produce standing waves, a wave driver was placed under the string, near the clamp, so that it could drive oscillations at specified frequencies. (Source: UCLA Physics 4AL Lab Manual, v. 20)

In order to produce three different wave speed measurements, three different weights were attached to the free end of the string that hung down from the pulley. The first weight had a

mass of  $99.8 \pm 0.1$  g, the second weight had a mass of  $200.2 \pm 0.14$  g, and the third weight had a mass of  $400.2 \pm 0.2$  g. The uncertainty in these measurements was based on uncertainty due to the scale that was used, as well as propagation of uncertainty based on counterweights.

The distance from the clamp to the top of the pulley was  $1432 \pm 1.4$  mm. Since a full wave cycle involved traveling along this distance twice, the length of travel “d” for the wave was  $2864 \pm 2.8$  mm.

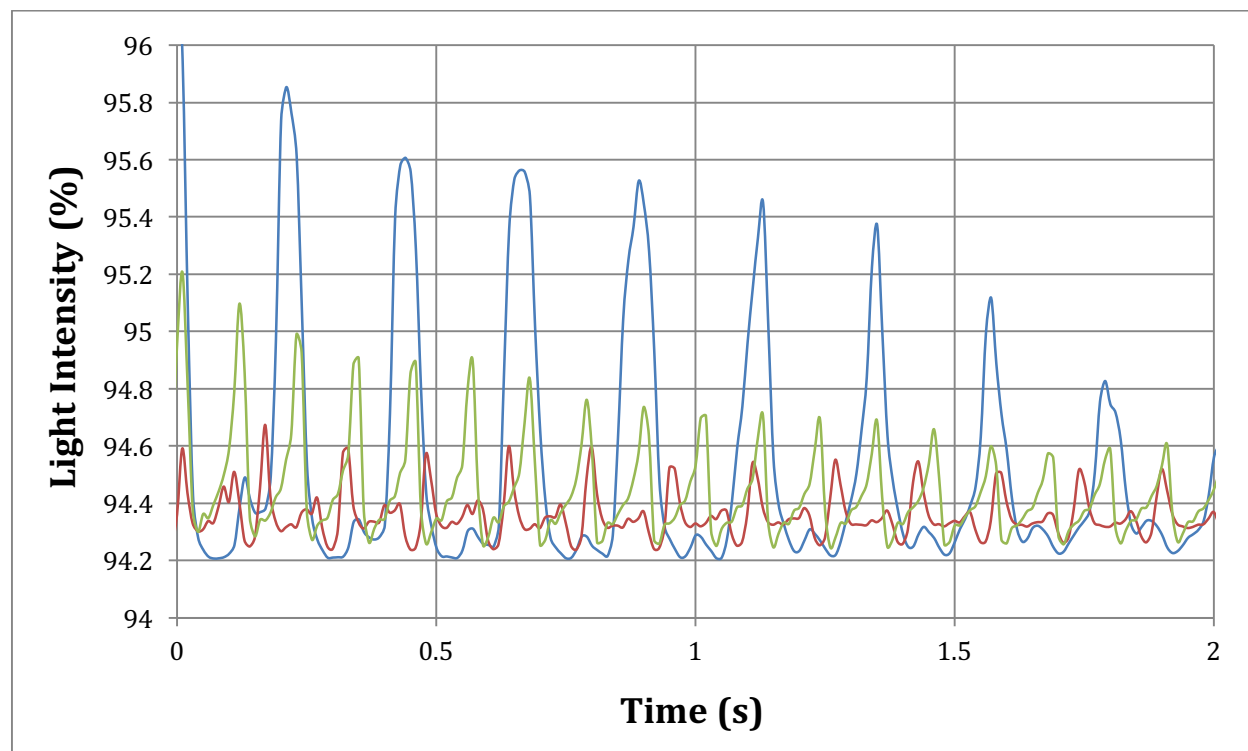


**Figure 2: Wave Pulses:** This graph shows wave pulse patterns based on 3 different linear mass densities, which correspond to the 3 masses that were hung from the string. The blue graph is based on the lightest mass that was used ( $99.8 \pm 0.1$  g), the red graph is based on the next lightest mass ( $200.2 \pm 0.14$  g), and the green graph is based on the heaviest mass that was used ( $400.2 \pm 0.2$  g). The masses that were used correlated with the frequency of pulses. An increase in mass caused an increase in wave frequency, and a decrease in mass caused a decrease in wave frequency.

Based on the wave data that is displayed in figure 2, it was possible to calculate the measured wave speed values for the 3 tensions by using equations 2.9 and 3.0. These values could be compared to the predicted wave speed values based on equations 2.6 and 2.8. The calculated values are shown in table 1.

Applied Mass (g)	$99.8 \pm 0.1$	$200.2 \pm 0.14$	$400.2 \pm 0.2$
Measured Wave Speed (m/s)	$12.7 \pm 0.2$	$18.2 \pm 0.2$	$25.7 \pm 0.2$
Predicted Wave Speed (m/s)	$12.044 \pm 0.004$	$16.908 \pm 0.004$	$24.033 \pm 0.004$

**Table 1: Measured and Predicted Wave Speeds:** This table displays the measured and predicted wave speeds according to the masses that were attached to the string. In all 3 cases, the measured value is higher than the predicted value, and the values do not fit within the uncertainty ranges of each other. Inaccurate measurements while recording the data may have led to this trend in the differences between predicted and measured values.

By comparing the measured and predicted wave speed values shown in table 1, it can be seen that the values do not agree with each other based on the given uncertainty ranges, and the measured values are all higher than the corresponding predicted values. Since this trend in the differences between measured and predicted values appears consistent, the differences may be due to systematic uncertainties involving inaccurate measurements that affected all data similarly.

In order to calculate a predicted frequency value of the fundamental node involving the mass of  $400.2 \pm 0.2$  g, it is possible to use equation 3.1 below, where “v” is the measured wave speed for the specified case, and “L” is the distance from the clamp to the apex of the pulley. The uncertainty can be calculated by using equation 3.2, which is based on the uncertainty of “v” and “L”. The predicted fundamental frequency “f” was found to be  $8.97 \pm 0.04$  Hz.

$$f = \frac{v}{2L} \quad (\text{Eq. 3.1})$$

$$\delta f = \frac{1}{2} |f_{best}| \sqrt{\left(\frac{\delta v}{|v_{best}|}\right)^2 + \left(\frac{\delta L}{|L_{best}|}\right)^2} \quad (\text{Eq. 3.2})$$

The frequency of the fundamental mode was measured in two ways. The first method involved using the Capstone software to monitor the photodiode signal amplitude. In this method, the driving frequency of the wave driver was set to the predicted frequency value of  $8.97 \pm 0.04$  Hz. The frequency was then tuned to find the frequency that corresponded to the largest signal amplitude from the photodiode. Since no noticeable change in amplitude was seen for frequency deviations of less than 0.001 Hz, the uncertainty in the measured frequency value was 0.001 Hz. The frequency of the fundamental mode based on the “maximum amplitude” method was found to be  $9.150 \pm 0.001$  Hz.

Another way to measure the frequency of the fundamental mode was to use the Lissajous figure method. In this method, the frequency was initially set to the predicted frequency value of  $8.97 \pm 0.04$  Hz, and a Lissajous figure was created based on the relationship between the output

voltage of the wave driver and the light intensity recorded by the photodiode. The frequency of the wave driver was then altered until a symmetrical Lissajous figure could be created with respect to the horizontal axis. The uncertainty in the measured frequency value was 0.005 Hz, since that is the largest frequency deviation that did not show a noticeable change in the Lissajous figures. By using the Lissajous figure method, the frequency of the fundamental mode was found to be  $9.195 \pm 0.005$  Hz. The corresponding Lissajous figure is shown in figure 3.

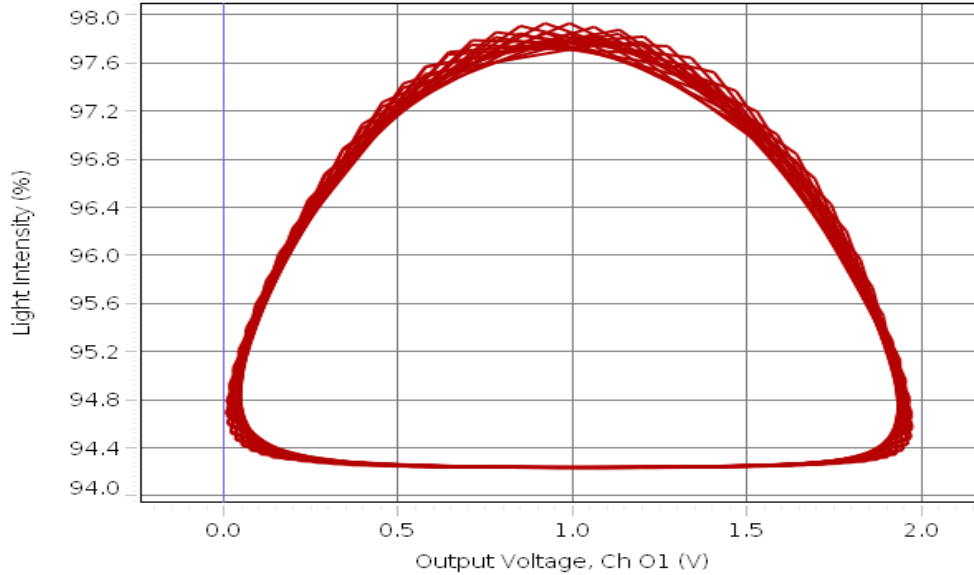


**Figure 3: Lissajous Figure for Fundamental Mode:** This is the Lissajous figure that was generated based on the frequency of the fundamental mode. The horizontal symmetry of the shape indicates that this measured frequency of  $9.195 \pm 0.005$  Hz is very close to the desired value. The uncertainty in this value is 0.005 Hz because that is the largest deviation in driving frequency that did not produce a noticeable change in the Lissajous figure.

The predicted frequency  $8.97 \pm 0.04$  Hz of the fundamental mode, and the measured values of  $9.150 \pm 0.001$  Hz and  $9.195 \pm 0.005$  Hz do not agree with each other based on the given uncertainty ranges. Although the measured values were relatively close, their differences may be due to the difficulty of creating a perfectly symmetrical Lissajous figure or ascertaining the frequency that produced the maximal photodiode signal amplitude. The larger differences between these measured frequencies and the predicted frequency may be due to imperfect placement of the wave driver and the laser pointer, which caused greater frequencies to be measured by the data acquisition system.

It is possible to predict the  $n^{\text{th}}$  mode frequencies by multiplying the predicted fundamental mode frequency by “n”. The calculated values for modes 2-5 are shown in table 2, along with the measured frequencies based on Lissajous figures shown in figure 4.



Mode	2	3	4	5
Predicted Frequency (Hz)	$17.94 \pm 0.08$	$26.9 \pm 0.1$	$35.9 \pm 0.2$	$44.9 \pm 0.2$
Measured Frequency (Hz)	$18.240 \pm 0.005$	$28.150 \pm 0.005$	$37.42 \pm 0.005$	$46.68 \pm 0.005$

**Table 2: Measured and Predicted Mode Frequencies:** This table shows predicted mode frequencies based on the predicted fundamental mode frequency of  $8.97 \pm 0.04$  Hz, along with measured mode frequencies obtained by creating symmetrical Lissajous figures. All of the measured frequencies larger than the corresponding predicted frequencies, and the values do not agree within the given uncertainty ranges, showing that sources of systematic uncertainty are likely responsible for the consistent trend in the differences between measured and predicted values.

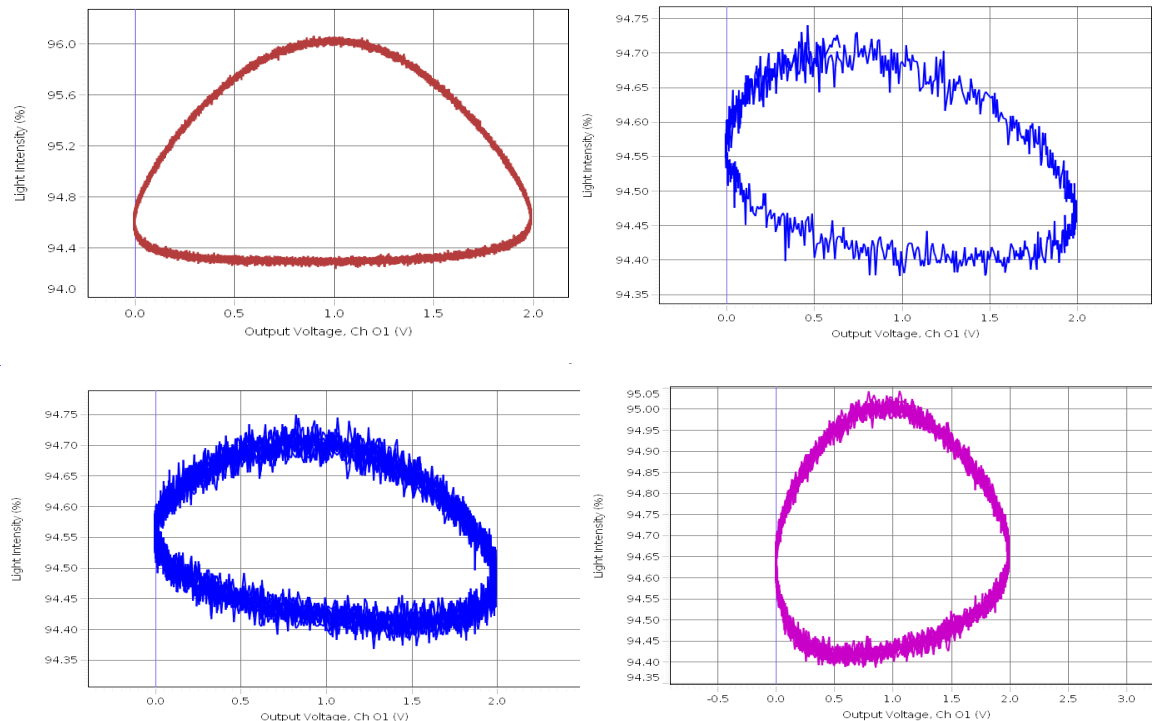


**Figure 4: Lissajous Figures for Modes 2-5:** These four images are the Lissajous figures corresponding to the measured mode frequencies of modes 2 (top-left), 3 (top-right), 4 (bottom-left), and 5 (bottom-right). As the mode frequency increased, it became more difficult to create symmetrical Lissajous figures, as seen in the figures based on modes 3-5.

Based on the measured and predicted mode frequencies shown in table 2, it can be seen that the frequency values do not agree with each other based on the given uncertainty ranges. There is a trend showing that the measured mode frequency is always greater than the corresponding predicted mode frequency. This may be due to the fact that the laser pointer and photodiode were not placed close enough to the top of the pulley, which caused the photodiode to record wave motion slightly earlier than expected.

## Conclusion

The purpose of this experiment was to examine the properties of waves as they propagate along a string, such as wave speed and mode frequency. After performing the experiment, data from tables 1 and 2 showed that the measured frequency values were consistently higher than predicted frequency values, and that the frequency values never agreed with each other based on their uncertainty ranges. Although this was the case, the differences in frequencies produced noticeable trends that indicated that sources of systematic uncertainty were the main causes of deviations rather than sources of statistical uncertainty. By taking more accurate measurements, and taking care to place sensors in the ideal locations, the differences in measured and predicted frequency values could be reduced.

One source of systematic uncertainty was due to inaccurate measurement of the length of the string. Since it was difficult to keep the string perfectly aligned with the ruler, it is likely that the string's length was not measured accurately, especially since the ruler had to be moved to measure long distances. If the measured length of the string was greater than the true value, the calculated mass density would be smaller, and the calculated wave speed would be larger. However, if the measured length of the string was smaller than the true value, the calculated mass density would be larger, and the calculated wave speed would be smaller. One way to eliminate this source of uncertainty would be to use a longer ruler that can be used to measure the full length of the string at the same time, as well as to have more people help keep the string aligned while measuring it.

Another source of systematic uncertainty was due to misplacement of the wave driver. If the wave driver was not placed close enough to the clamp, the generated waves may not have traveled along the full length from the clamp to the apex of the pulley. If the wave driver were moved further away from the clamp, the generated waves would have traveled shorter distances along the string, causing larger frequencies and wave speeds to be measured. One way to eliminate this source of uncertainty would be to move the wave driver as close to the clamp as possible so that the waves are allowed to travel along the full length of the string.

## Extra Credit

By using the Lissajous method, it was seen that the highest mode that could be found was the 13<sup>th</sup> mode. After the 13<sup>th</sup> mode, it was extremely difficult to create a symmetrical Lissajous figure. At the 60<sup>th</sup> mode, which has a predicted frequency of  $538.2 \pm 2.4$  Hz, the wave driver mainly produced audible sound. The determination of the frequency for each mode is shown in table 3 below.

Mode	1	2	3	4	5	6	7
Frequency (Hz)	$9.195 \pm 0.005$	$18.240 \pm 0.005$	$28.150 \pm 0.005$	$37.42 \pm 0.005$	$46.680 \pm 0.005$	$54.270 \pm 0.005$	$63.965 \pm 0.005$
Mode	8	9	10	11	12	13	
Frequency (Hz)	$73.155 \pm 0.005$	$82.005 \pm 0.005$	$92.125 \pm 0.005$	$101.820 \pm 0.005$	$110.285 \pm 0.005$	$120.145 \pm 0.005$	

**Table 3: Frequencies of Modes 1-13:** This table shows the frequencies of modes 1-13 based on the generated Lissajous figures. After the 13<sup>th</sup> mode, it was difficult to generate a symmetrical Lissajous figure since very small vibrations were produced along the string.

The distance between the laser spot and the top of the pulley was  $52 \pm 1$  mm. The first mode that will produce a node at this position can be found by dividing the distance from the clamp to the top of the pulley by  $52 \pm 1$  mm. This shows that a node would be produced if  $n = 27.5$ . However, since modes are found in terms of whole numbers, this number should be doubled to give the 55<sup>th</sup> mode, which corresponds to a frequency of  $493.4 \pm 2.2$  Hz. Since setting the wave driver to frequencies this high mainly produces noise, it would be difficult to take data measurements at modes near this one.